

Simulation of Laser-wires at CLIC using BDSIM

Grahame A. Blair, Royal Holloway Univ of London, UK.

Abstract

A laserwire system within the CLIC beam delivery system is simulated using Geant4. The issues of extracting the signal in the presence of beam-related backgrounds is addressed.

1 INTRODUCTION

In the linear collider (LC) beam delivery system (BDS), the properties of the electron/positron beams at the exit of the main linac and also along the BDS will need to be measured in order to understand the beam optics and provide sufficient diagnostics for luminosity optimisation. This information must be fed back in real time if it is to be effective during machine operation, so a fast and accurate beam profile monitor is needed. The use of Compton scattering of laser light off the incoming electron/positron beams is one device (called a laser-wire) currently being proposed to measure the transverse lepton beam profile in the BDS. The principles of laser-wire operation are outlined in more detail in Sec. 2.

While the principle of operation of a laser-wire has been demonstrated at the SLC [1, 2] and is currently producing nice results at the KEK ATF facility [3] and first studies at the CLIC CTF2 [4], the use of a laser-wire in a realistic LC BDS has yet to be demonstrated. In addition to the challenge of scanning the electron beam rapidly and accurately (the subject of ongoing R&D [5]), there is the issue of extracting the Compton scattered photons and/or leptons. A detailed simulation program, BDSIM [6] based on GEANT4 [7] has been developed to study electron/positron tracking, collimation, muon production and the backgrounds associated with secondaries from showers produced when primary beam or halo particles strike apertures along the BDS. The program also allows the tracking of the Compton-scattered laser-wire electrons and photons and so is ideally suited to studying the operation of a laser-wire within a realistic BDS, including the effects of backgrounds and limitations of beam-line apertures. A first such study, performed for the nominal long CLIC 1.5 TeV BDS [8], is outlined in Sec. 3. In this study the effects of backgrounds due to halo are discussed in some detail and it is shown that the observation of signal over background may require careful optimisation of the location of the laser-wire with respect to the BDS collimation system. A related study [9] also shows that extraction of the Compton-scattered particles may be challenging.

2 PRINCIPLES OF THE LASER-WIRE

A very good introduction to the principle and theory of laser-wires can be found in Ref. [2]. For completeness, some of the key results are reviewed here and referred to later in the discussion of detailed simulation.

The Compton cross section σ_C is related to the Thomson scattering cross section $\sigma_0 = 6.65 \times 10^{-25} \text{cm}^2$ by Eqn. 1:

$$\sigma_C = \sigma_0 \frac{3}{4} \left\{ \frac{1+\epsilon}{\epsilon^3} \left[\frac{2\epsilon(1+\epsilon)}{1+2\epsilon} - \ln(1+2\epsilon) \right] + \frac{1}{2\epsilon} \ln(1+2\epsilon) - \frac{1+3\epsilon}{(1+2\epsilon)^2} \right\} \quad (1)$$

where $\epsilon = \gamma \frac{\omega_0}{m_e}$ is the normalised energy of the laser photons in the electron rest frame and γ is the Lorentz factor associated with the incident electron beam energy E_b ($\gamma = \frac{E_b}{m_e}$). The energy spectrum of the emerging gamma rays is given by Eqn. 2:

$$\frac{d\sigma}{d\omega} = \frac{3\sigma_0}{8\epsilon} \left\{ \frac{1}{1-\omega} + 1 - \omega + \left[\frac{\omega}{\epsilon(1-\omega)} \right]^2 - \frac{2\omega}{\epsilon(1-\omega)} \right\} \quad (2)$$

In the following we consider an electron bunch with a Gaussian distribution of particles in the plane transverse to the bunch velocity, as illustrated in Fig. 1. The transverse dimension we are interested in measuring is σ_b , which must be aligned perpendicular to the direction of the laser beam. The setup is illustrated in Fig. 1(a). The laser beam is focused to a small spot Gaussian spot size of with waist (RMS size) σ_f which, for a diffraction-limited laser beam is given by

$$\sigma_f = \frac{\lambda f_\ell}{4\pi\sigma_\ell} \quad (3)$$

where f_ℓ is the focal length of the optics which is focusing the laser down to the small spot size and σ_ℓ is the RMS spot size of the beam when it leaves the laser. The useful depth z_R (the Raleigh range) of laser beam is given by Gaussian beam optics to be:

$$z_R = \frac{4\pi\sigma_f^2}{\lambda}. \quad (4)$$

We will require that the laser pulse lasts longer than the time taken for one bunch to pass through it. In the case of CLIC the 30 μm RMS bunch lengths will require minimum laser pulse lengths of approximately 100 fs, synchronised with the electron bunch. Now that the entire electron bunch sees the laser beam, the number of Compton photons per electron bunch is given by:

$$N_\gamma = N_b \frac{P_L \sigma_C \lambda}{c^2 h} \frac{1}{\sqrt{2\pi}\sigma_s} \exp\left(\frac{-y^2}{2\sigma_s^2}\right) \quad (5)$$

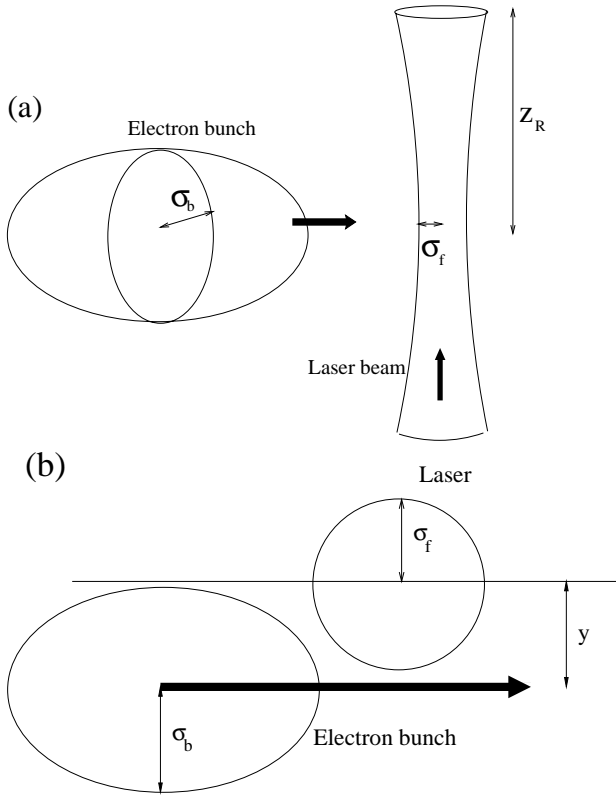


Figure 1: Setup showing the definition of the laser beam and beam spot dimensions relevant to this analysis. (a) Shows a side view; note that it is the dimension of the beam spot perpendicular to the laser beam that is denoted by σ_b . (b) View from the top, showing an offset y between the centre of the bunch and the centre of the laser beam.

where N_b is the number of electrons per bunch, $\sigma_s^2 \equiv \sigma_b^2 + \sigma_f^2$ and y is the relative transverse offset between the bunch and the laser spot as illustrated in Fig. 1(b).

In the following we evaluate the maximum rate of Compton events at $y = 0$ assuming a diffraction limited laser waist and a nominal transverse electron cross-section of $10 \mu\text{m}$ and a representative optical focal length of 20 cm with in incoming laser beam of size $\sigma_\ell = 1 \text{ cm}$. The resulting cross-sections for the range of energies relevant to a linear collider are shown in Tab. 1, together with the number of Compton events, N_C , for a nominal 10^{10} incident electrons and a Q-switched laser-power of 100 MW per pulse for IR photons, scaled approximately for shorter wavelengths, under the assumption that the laser-beam spot size is smaller than the electron bunch profile at the point of overlap. Higher effective laser powers can be obtained using mode-locked lasers with ps-pulses timed accurately to coincide with the electron bunches. For the following studies, a nominal 1000 Compton scatters are used as a nominal laser-wire event assuming a laser wavelength of 532 nm. Several such events would be part of a single laser-wire profile scan and several such scans may be required for a single electron bunch profile measurement;

however for the point of discussion the use of 1000 Compton scatters per laser shot is justified by the numbers in Tab. 1 for $\lambda = 532 \text{ nm}$. Note that the numbers in the table are the maximum, when electron and laser are aligned. The number of Compton events will decrease either side of the central values, as the Gaussian electron bunch profile is scanned.

Electron Energy (GeV)	Laser Wavelength (nm)	Pulsed Laser Power (MW)	Cross Section (10^{-25} cm^2)	N_C
250	1064	100	2.73	19200
250	532	50	1.98	3510
250	355	25	1.60	950
250	266	10	1.36	242
500	1064	100	1.98	13900
500	532	50	1.36	2414
500	355	25	1.06	629
500	266	10	0.880	157
1500	1064	100	1.06	7450
1500	532	50	0.668	1186
1500	355	25	0.500	297
1500	266	10	0.404	72
2500	1064	100	0.758	5330
2500	532	50	0.463	822
2500	355	25	0.341	202
2500	266	10	0.273	49

Table 1: Representative laser-wire cross-sections and total number of events for some nominal laser-powers and for 10^{10} electrons. Higher laser powers could be obtained using mode-locked systems. N_C is the number of Compton events when the laser is at the centre of the electron bunch.

3 LASER-WIRE SIMULATION

As described in the introduction, BDSIM is a program that incorporates efficient accelerator-style tracking (based on transfer matrix techniques) with the detailed shower generation and physics processes of Geant4 [7], the modern standard for particle physics simulation. More details are provided in Ref. [6]. BDSIM includes a laser-wire process that generates the appropriate Compton-scattered lepton and photon for an incoming electron interacting with a laser beam, with resulting energy distributions derived from Eq. 2 and shown in Fig. 4. The wavelength and also the direction of the laser beam can be specified in the program, but in the following the direction is fixed perpendicular to the lepton beam. Either the scattered electron only, or the photon only, or both the electron and the photon can be tracked further down the BDS. This allows the position of the laser-wire to be optimised and enables a study of the best way to extract the signal. A first such study is described in the following.

In order to illustrate the use of BDSIM for a realistic BDS laser-wire, the laser beam was situated just after the first energy spoiler in the long baseline design [8], at $z=1146 \text{ m}$. The x and y spatial distributions of electrons at the laser-wire are shown in Fig. 2. Clearly the challenge is to measure the transverse width in y , which for CLIC will mean accuracies of order a few μm . The laser-wire position chosen here is a point of high dispersion for energy E with $\frac{\partial E}{\partial x} = -3740 \text{ GeV m}^{-1}$. The distribution of E against x is shown in Fig. 3 (left) and the distribution of the value $(E - 1500) + 3740 \times x$ is shown in Fig. 3 (right). If the

laser-wire were to be used to measure the energy spread in the beam, then this distribution shows that the intrinsic accuracy of this method is about 170 MeV, to be added in quadrature to the factor $3740 \times \Delta x$ where Δx is the accuracy on the endpoints of the x -distribution measured with the laser-wire. To be comparable with the intrinsic resolution, the laser-wire would need an accuracy from a scan of order $0.17/3740 \text{ m} = 45 \mu\text{m}$, well within the laser-wire capabilities discussed below. Of course, several scans could be used to increase the statistical power of the measurement, so accuracies of CLIC energy spread measurement at the level of 10^{-4} seem achievable.

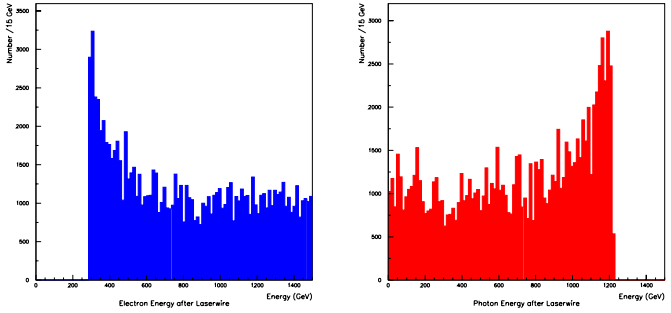


Figure 4: The energy distributions for electrons (left) and photons (right) after Compton scattering in the laser-wire.

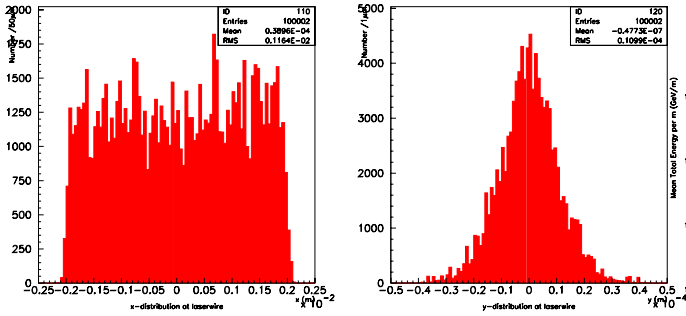


Figure 2: The initial spatial x (left) and y (right) distributions at the point of the laser-wire for this study. The flat x -distribution (left) is due to the fact that the position chosen is in a region of high dispersion, close to the first energy spoiler.

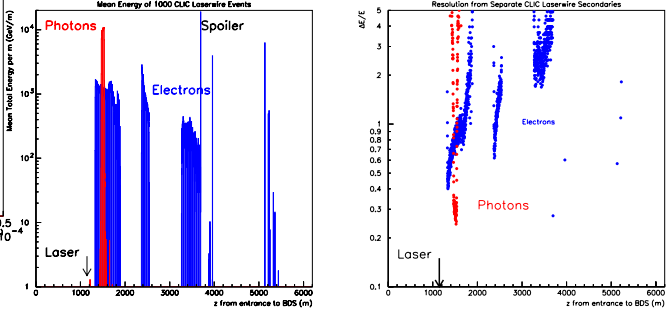


Figure 5: Left: the energy distribution along the BDS resulting from 1000 Compton scatters. Shown in red (light grey) are the energy deposits per m from the scattered photons and in blue (dark grey) the energy deposits from the scattered electron. The laser wavelength used in these studies is 532 nm. Right: the intrinsic relative fluctuations in the energy deposits arising from the Compton process as a function of position along the BDS.

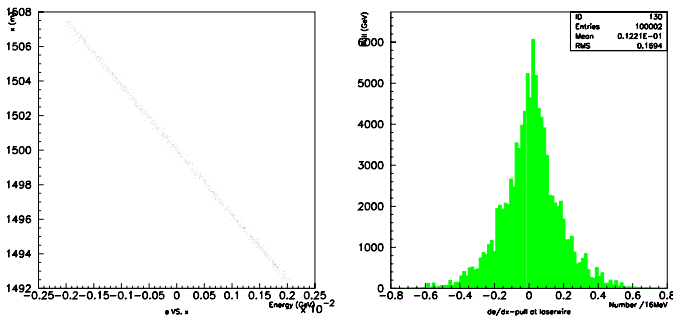


Figure 3: The initial distribution of energy against x -position (left) and the pull distribution (right) given by $(E - 1500) + 3740 \times x$ at the point of the laser-wire for this study.

One of the major challenges of a laser-wire system is to extract the Compton photons, or electrons, in an already crowded BDS. At the point of the laser-wire, the energy distributions are shown in Fig. 4 for the scattered electrons (left) and the photons (right). These particles were subsequently tracked using BDSIM and the resulting energy deposition as a function of length along the BDS is displayed in Fig. 5 (left).

In the BDS the profile measurement will be made by measuring the total energy in a calorimeter stationed somewhere along the beam-line. By firing 100 laser-wire events, each of 1000 Compton scatters, the fluctuations in the signal between events can be determined. The results are shown in Fig. 5 (right). Here it can be seen that the fluctuations are large because the energy of the event is scattered over a long region. This effect would severely limit the intrinsic performance of the laser-wire which, if it is to provide a fast and accurate profile measurement, needs to make use of as much of the scattered energy as possible.

A potential solution to this problem could be provided by installing dedicated calorimeters close to the beam, assuming that issues such as radiation hardness and wake field generation could be overcome. The above case of a laser installed just after the first energy collimator (at $s=1146$ in the baseline 1.5 TeV BDS) was explored to see how the Compton-scattered electron and photon distributions evolve further down the BDS. The situation at a location $s=1471 \text{ m}$, *i.e.* 325 m after the laser-wire, is shown in Fig. 6

(left).

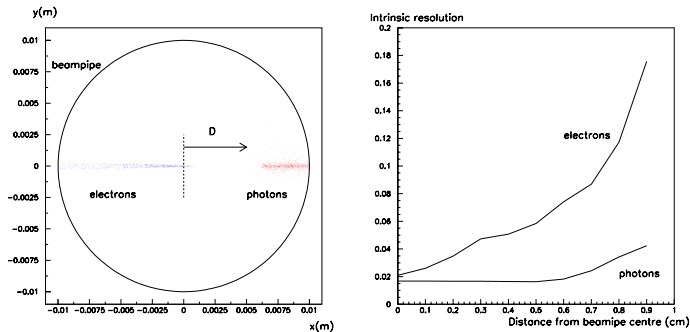


Figure 6: Left: the spatial distribution of 1000 Compton-scattered electrons (blue/dark grey) and photons (red/light grey) 325 m after the laser-wire. The distance D for photons (and $-D$ for the electrons) is used to investigate the optimal position of a beam-pipe calorimeter. Right: the intrinsic resolution that could be achieved by capturing all the energy at distances greater than D for electrons and positrons.

If a calorimeter (e.g. a radiation-hard crystal of lead tungstate) were positioned with one edge at distance D , then the intrinsic resolution can be estimated by summing the energy from electrons and photons at distances greater than D . The results shown as a function of D for photons (and $-D$ for electrons) are presented in Fig. 6 (right). Clearly the best resolution can be obtained from using the photons, where a calorimeter placed at, say, 0.5 cm from the beam could in principle yield measurements at the 2% level, before effects of energy leakage and detector resolution are included. The latter effects, together with full simulation of a candidate calorimeter, will need to be investigated in a future study. However the conclusion of the work presented here is that simply using energy-loss monitors along beam-line will not provide sufficient accuracy (at best of order 30% per event from Fig. 5 (right)) to provide a fast beam profile measurement and so dedicated calorimetry needs to be considered.

4 HALO STUDIES

The beam halo accompanies the electron/positron bunch and contains particles with a much greater phase-space volume than those of the core bunch. For the purposes of this study, the halo was defined by uniform distributions in phase-space variables according to the parameters defined in Tab. 2. Particles distributed according to this phase space were tracked along the baseline 6 km CLIC BDS [8] and their resulting energy deposition along the BDS, together with their contribution to the background of the laser-wire Compton measurements estimated using BDSIM.

Some preliminary results are shown in Fig. 7 (left) where the energy loss due to 10^5 halo particles is shown and the plot is normalised to be equivalent to a beam halo with

Bunch parameter	Range
x	$10. \times 1.25 \times \sigma_x$
y	$70. \times 1.25 \times \sigma_y$
x'	$10. \times 1.25 \times \sigma_x$
y'	$70. \times 1.25 \times \sigma_y$
E	$(0.98 - 1.02) \times E_0$

Table 2: Parameters defining flat distributions to describe the CLIC beam halo

bunch charge 10^{-3} of the nominal bunch charge of 4×10^9 . Most of the particles are absorbed in the spoilers (consisting of one radiation length of graphite) and absorbers (consisting of 35 cm of copper); however additional losses due to synchrotron radiation or other particles leaving the beam-pipe are also apparent. A cut of 10 GeV was applied to charged particles in the EM showers.

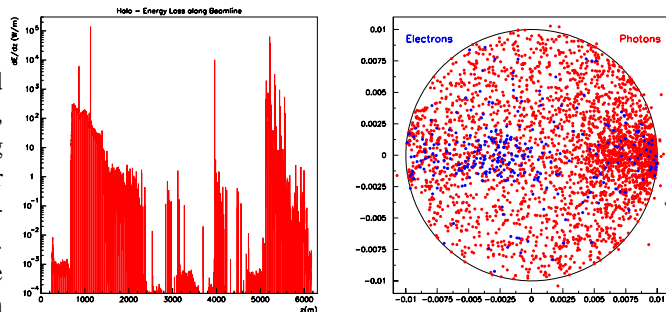


Figure 7: Left: the total energy loss per bunch train for the halo described in Tab. 2 as a function of position along the BDS for the CLIC long baseline design. 10^5 initial halo particles were used in this simulation and the normalisation in this plot assumes that the halo is 10^{-3} of the nominal bunch charge of 4×10^9 . Right: the spatial distribution of halo particles (electrons blue/dark grey and photons red/light grey) tracked 320 m downstream of the laser-wire position. Only 1000 halo particles were tracked; a halo of 10^{-3} of the nominal bunch occupancy of 4×10^9 , would lead to $\sim 4 \times 10^6$ halo particles; a factor 4×10^3 greater than shown here.

A quick run of 1000 halo events ($\sim 1.6 \cdot 10^{-6}$ of the halo of one pulse train of 154 bunches), tracking the halo downstream of the collimators, gives the spatial distribution shown in Fig. 7 (right) with corresponding energy distributions given in Fig. 8 for those particles to the left ($x < 0$) and right ($x > 0$) inside the beam-pipe.

For photons: signal ($\sim 7 \cdot 10^5 \times 154$) GeV= 10^8 GeV per train compared to halo $\sim 1.2 \times 10^5 / (1.6 \times 10^{-6}) = 7 \cdot 10^{10}$ GeV per train. So the signal is completely swamped by background in this region, with signal/background $\sim 10^{-3}$.

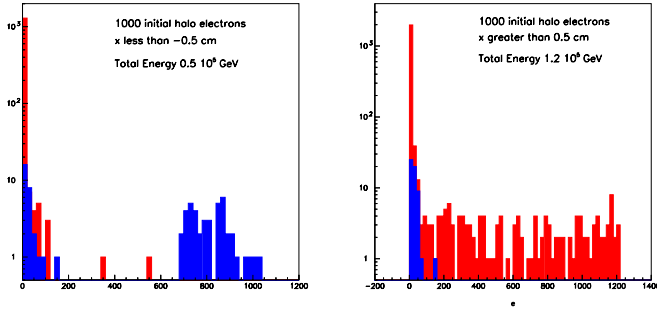


Figure 8: Energy distributions of halo particles tracked 320 m downstream of the laser-wire position Left: particles to the left of Fig. 7. Right: those to the right of Fig. 7. Only 1000 halo particles were used for this study. In the figure, the contributions from electrons are shown in blue/dark grey and from photons in red/light grey.

5 CONCLUSIONS

Laser-wire R&D is progressing well with accelerator facilities worldwide installing and optimising these devices. While many technological challenges remain to focus and scan the electron bunches rapidly and accurately, the issues of where to locate the laser-wires and how to extract the resulting Compton-scattered particles in a realistic BDS are only now starting to be addressed. A first study was presented here, using full simulations, that assumed a laser-wire location in the collimation region of the BDS; a natural location because this is where the lepton beams have their largest cross-section (large beta-functions). However, this is also where the backgrounds will be large due to secondaries from the halo particles that shower in the collimators. As shown here, these backgrounds can completely swamp the laser-wire signal, under somewhat pessimistic assumptions of the halo occupancy.

More study is clearly required. However this first look at the laser-wire location and background issues suggests that the incorporation of laser-based beam diagnostics in the BDS is something that needs to be addressed integrally in the BDS design and not something added later. Indeed dedicated diagnostics sections may be necessary, well isolated from the collimation regions, if the technique is to work.

6 ACKNOWLEDGEMENTS

I have benefited from many useful discussions with J. Apostoliakis, H. Burkhardt, D. Schulte, N. Walker, F. Zimmermann. I am very grateful to the CERN CLIC group for financial support and hospitality throughout the development of BDSIM and for financial support from DESY for the simulation studies reported here. Additional support is acknowledged from the Royal Society, the British Council ARC programme and INTAS grant No 00-00679.

7 REFERENCES

- [1] R. Alley *et al.* Nucl. Instr. Meth. **A379**:363–365, 1996.
- [2] P. Tenenbaum, T. Shintake SLAC-PUB-8057 (1999)
- [3] Y.Honda *et al.*, this workshop.
- [4] T.Lefevre *et al.*, this workshop.
- [5] “R&D Towards a Laser Based Beam Size Monitor for the Future Linear Collider” T. Kamps, G. A. Blair, F. Poirier, H. C. Lewin, S. Schreiber, N. Walker, K. Wittenburg , Proc. EPAC02, Paris 2002.
- [6] G .A Blair, “Simulation of the CLIC Beam Delivery System using using BDSIM”, CLIC Note 509 (2002).
- [7] GEANT4 collaboration, S. Agostinelli *et al.*. “GEANT4 - A Simulation Toolkit” (SLAC-PUB-9350, to be published in NIM, 2002.)
- [8] R. Aßmann, H. Burkhardt, S. Fartoukh, J. B. Jeanneret, J. Pancin, S. Redaelli, T. Risselada, F. Zimmermann, H.-J. Schreiber, “Overview of the CLIC Collimation Design”, IEEE PAC2001, Chicago (2001); CLIC Note 493 (2001).
- [9] G. Penn, this workshop.